JACS
JOURNAL OF THE AMERICAN CHEMICAL SOCIETY

Article

pubs.acs.org/JACS

Chemical and Structural Analysis of an Antibody Folding Intermediate Trapped during Glycan Biosynthesis

Thomas A. Bowden,*[,†,⊥] Kavitha Baruah,[‡,⊥] Charlotte H. Coles,[†,⊥] David J. Harvey,[‡] Xiaojie Yu,[‡] Byeong-Doo Song,[§] David I. Stuart,[†,∥] A. Radu Aricescu,[†] Christopher N. Scanlan,[‡] E. Yvonne Jones,[†] and Max Crispin*[,‡]

[†]Division of Structural Biology, University of Oxford, Wellcome Trust Centre for Human Genetics, Roosevelt Drive, Oxford OX3 7BN, United Kingdom

[‡]Oxford Glycobiology Institute, Department of Biochemistry, University of Oxford, South Parks Road, Oxford OX1 3QU, United Kingdom

[§]Scripps Korea Antibody Institute, 192-1 Hyoja-dong, Chuncheon, Gangwon 200-701, Korea

[∥]Science Division, Diamond Light Source Ltd., Diamond House, Harwell Science and Innovation Campus, Didcot, Oxfordshire OX11 0DE, United Kingdom

Supporting Information

ABSTRACT: Human IgG Fc glycosylation modulates immunological effector functions such as antibody-dependent cellular cytotoxicity and phagocytosis. Engineering of Fc glycans therefore enables fine-tuning of the therapeutic properties of monoclonal antibodies. The N-linked glycans of Fc are typically complex-type, forming a network of noncovalent interactions along the protein surface of the Cγ2 domain. Here, we manipulate the mammalian glycan-processing pathway to trap IgG1 Fc at sequential stages of maturation, from oligomannose- to hybrid- to complex-type glycans, and show that the Fc is structurally stabilized following the transition of glycans from their hybrid- to complex-type state. X-ray crystallographic analysis of this hybrid-type intermediate reveals that N-linked glycans undergo conformational changes upon maturation, including a flip within the trimannosyl core. Our crystal structure of this intermediate reveals a molecular basis for antibody biogenesis and provides a template for the structure-guided engineering of the protein−glycan interface of therapeutic antibodies.

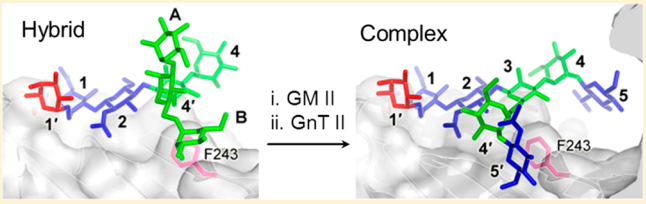

INTRODUCTION

Antibodies are multifunctional glycoproteins, able to bind antigens through variable Fab domains and cellular receptors via the constant Fc region. This dual functionality enables the recruitment of the cellular immune system to sites of infection by antibody-dependent cellular cytotoxity (ADCC) and antibody-dependent cellular phagocytosis (ADCP), and can lead to the localized activation of the complement system. Glycan and protein engineering of the Fc domain can generate therapeutic monoclonal antibodies with tailored receptor binding functionality.[1,2] In contrast to chemical and chemo-enzymatic methods to modulate glycan structures,[3−9] we use glycosidase inhibitors and a cell line deficient in a glycosyltransferase to generate antibody glycoforms containing specific carbohydrate structures.

The Fc region of immunoglobulin G (IgG) is a homodimer consisting primarily of heavy chain Cγ2 and Cγ3 domains. The C-terminal Cγ3 domain protomers interact through an extended protein−protein interface, occluding over 1100 Å^2 of protein surface,[10] and adopt rigid conformations that exhibit little structural variation.[11] In contrast, the Cγ2 domain protomers have only been observed to interact via glycan−glycan contacts between opposing N-linked chains at Asn297.[11−13] Glycan-mediated maintenance of the spacing between the Cγ2 domains is critical for cellular Fcγ receptor (FcγR) binding, which occurs asymmetrically at the tip of the Cγ2 domains and lower hinge region.[14] Deglycosylation, for example, by bacterial endoglycosidases, leads to disruption of Cγ2 spacing and significantly impairs FcγR binding.[15,16]

The impact of Asn297 glycosylation upon Fc structure is not limited to influencing Cγ2 spacing. IgG Fc glycosylation also stabilizes the protein through an approximately 500 Å^2 glycan−protein interface along the surface of the Cγ2 domain.[11,13,17] These glycan−protein contacts are believed to limit both the processing by Golgi-resident glycosyltransferases and the conformational freedom of the glycan.[18] This model is supported by an NMR study, which proposes that Fc glycans exist in an equilibrium with an approximately equal proportion of a "free" state, with highly mobile glycans, and a less mobile "bound" state, observable by X-ray crystallography, with

Received: June 21, 2012
Published: October 1, 2012

dx.doi.org/10.1021/ja306068g | J. Am. Chem. Soc. 2012, 134, 17554−17563

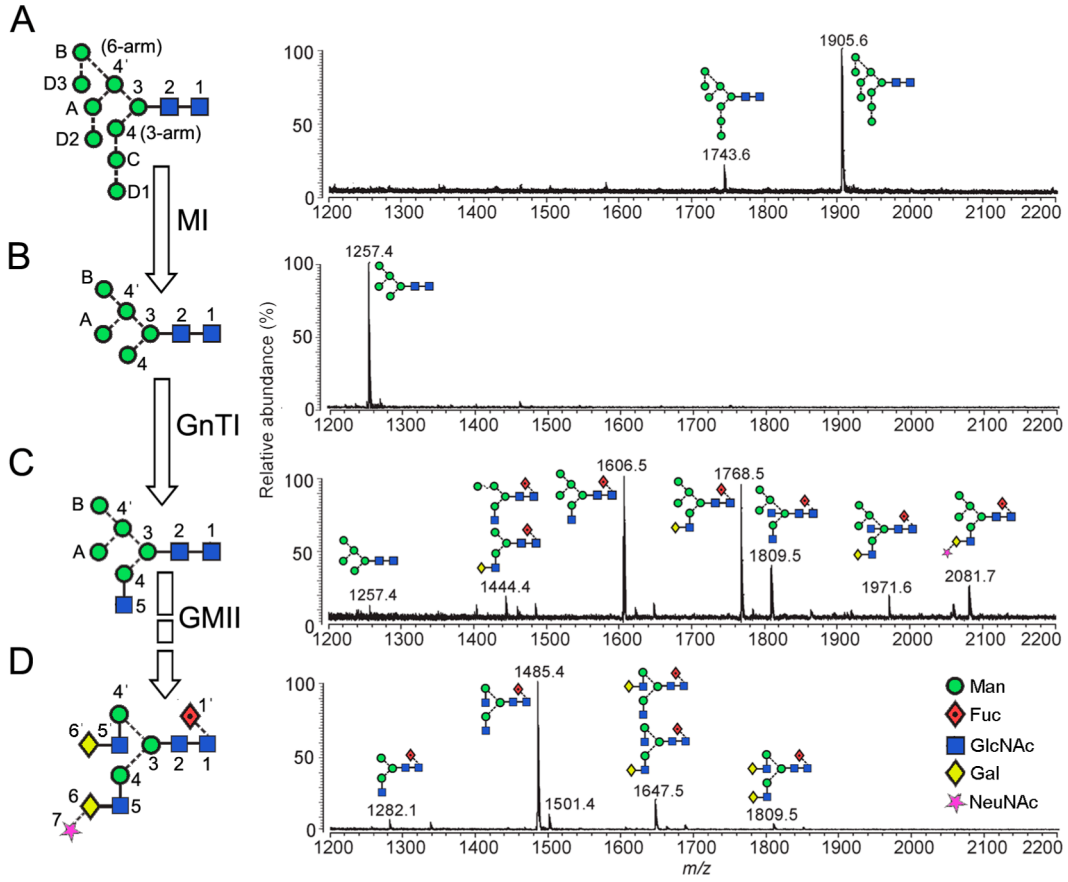

Figure 1. The N-linked glycosylation processing pathway (left) and MALDI-TOF MS analysis of associated IgG1 Fc glycoforms (right). Following protein folding and hydrolysis of the glucose cap, glycoforms were isolated by stalling the pathway at sequential stages of biogenesis. (A) The $Man_9GlcNAc_2$ glycoform resulted from α-mannosidase (MI) inhibition with kifunensine. (B) The $Man_5GlcNAc_2$ glycoform resulted from expression in a GlcNAc transferase (GnT) I-deficient cell line. (C) Hybrid-type glycosylation resulted from expression in the presence of the Golgi α-mannosidase II (GMII) inhibitor, swainsonine. (D) Complex-type glycosylation resulted from activity of Golgi-resident glycosyltransferases. Ions are $[M + Na]^+$. The sialylated glycan is also present as a sodium salt. The following symbols were used to represent glycans[33] and are shown as a key in panel D: yellow ♦, galactose; blue ■, GlcNAc; green ●, Man; red ♦ with black dot, fucose; pink ★, sialic acid. Linkage positions are shown by the angle of the lines linking the sugar residues (vertical line, 2-link; forward slash, 3-link; horizontal line, 4-link; back slash, 6-link). Anomericity is indicated by unbroken lines for β-bonds and broken lines for α-bonds.

ordered protein−glycan interactions less accessible to enzymatic processing.[19]

The composition of IgG Fc glycans is largely directed by the protein.[18,20] The glycosylation exhibits limited processing and consists of a predominantly biantennary complex-type framework with partial occupancy of galactose, core α1→6-linked fucose, low levels of "bisecting" GlcNAc, and sialic acid.[18] This limited processing is in contrast to the highly sialylated complex-type glycosylation typically observed on secreted glycoproteins.[18]

The human FcγRs (FcγRI, FcγRIIa, FcγRIIb, and FcγRIIIa) display binding properties dependent upon the presence and composition of the Fc glycan.[1] For example, afucosylated antibody glycoforms, which may find utility in anticancer treatment, are inflammatory and exhibit enhanced ADCC due to elevated binding to the activatory FcγRIIIa.[21] In contrast, anti-inflammatory IgG glycoforms display increased levels of terminal sialylation and are under investigation for enhanced intravenous immunoglobulin therapy.[22]

Biosynthetic Fc precursors have also been investigated for therapeutic applications due to their altered FcγR-dependent effector functions.[9,23−26] Monoclonal antibodies found in the early steps of carbohydrate maturation including oligomannose- or afucosylated hybrid-type glycans, for example, display increased affinity for FcγRIIIa and enhanced ADCC functionality,[24,26] albeit with potentially elevated serum clearance.[27,28] Here, we have generated and characterized a panel of such glycoform intermediates and present the crystal structure of the key precursor bearing hybrid-type glycosylation. In the context of the biosynthetic pathway of N-linked carbohydrates, this glycoform represents the intermediate formed between the immature oligomannose and the native, complex-type states.[29] This Fc glycoform, generated by recombinant mammalian protein expression in the presence of the Golgi α-mannosidase II inhibitor, swainsonine,[30,31] was crystallized and subjected to X-ray crystallographic analysis to 2.4 Å resolution. Examination of this structure reveals a novel interaction between carbohydrate and protein components. Together with thermostability analyses, the structure provides a model for the conformational transitions that IgG Fc undergoes upon glycoprotein maturation and provides a template for the structure-guided engineering of therapeutic antibodies.

■ RESULTS AND DISCUSSION

Expression and Purification of IgG Fc Glycoforms. A panel of IgG1 Fc glycoforms, corresponding to key stages of the

dx.doi.org/10.1021/ja306068g | J. Am. Chem. Soc. 2012, 134, 17554−17563

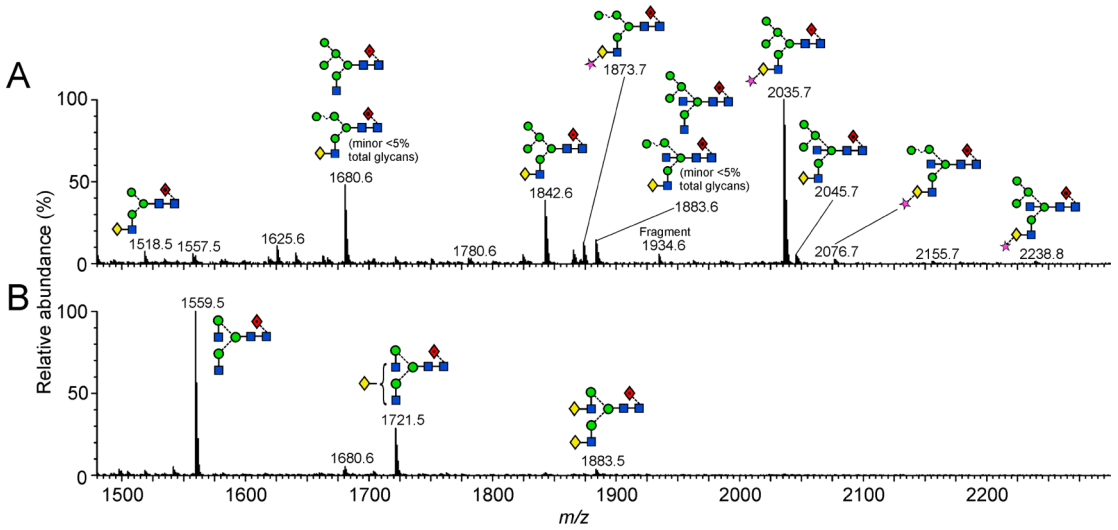

Figure 2. Negative ion electrospray mass spectra of recombinant IgG1 Fc N-linked glycans following expression in the (A) presence and (B) absence of the Golgi α-mannosidase II inhibitor, swainsonine. Neutral glycan ions are $[M + H_2PO_4]^-$, sialylated glycans are $[M - H]^-$. Symbols for the structures are as described in Figure 1. Isomeric assignments were determined by ESI–MS/MS (Figure 3). The presence of a minor population of Man_4-based hybrids was detected in the fragmentation spectra by very low abundance $^{1,3}A_3$ ions at m/z 424 (Figure 3B,D).

mammalian N-linked biosynthesis after calnexin/calreticulin-mediated protein folding,[29,32] was generated using either a lectin-resistant cell line deficient in glycosyltransferase activity or by the use of glycosidase inhibitors (Figure 1).

We isolated IgG1 Fc bearing $Man_9GlcNAc_2$, $Man_5GlcNAc_2$, hybrid-, and complex-type glycan structures. These glycoforms are generally representative of the carbohydrates appearing in the ER, and the early, medial, and late Golgi apparatus, respectively.[29,34]

Glycan Analysis. The N-linked glycosylation of each Fc glycoform was assessed by positive ion matrix-assisted laser desorption/ionization (MALDI) time-of-flight (TOF) mass spectrometry (MS) of enzymatically released glycans (Figure 1). Expression of Fc in the presence of the ER and Golgi α1→2-mannosidase inhibitor, kifunensine, resulted in a largely homogeneous $Man_9GlcNAc_2$ glycan (m/z = 1905.6; Figure 1A) with limited processing to the $Man_8GlcNAc_2$ derivative (m/z = 1743.6; Figure 1A). Expression of the Fc region in GnT I-deficient human embryonic kidney (HEK) 293S cells[35] resulted in a similarly homogeneous spectrum dominated by $Man_5GlcNAc_2$ glycans (m/z = 1257.4; Figure 1B).

The next glycoform in the N-linked biosynthetic pathway, the hybrid-type glycan, was isolated using the Golgi α-mannosidase II inhibitor, swainsonine. Swainosine prevents hydrolysis of the Man**A** and Man**B** saccharides of the "6-arm" of the trimannosyl core.[30,31] However, this inhibition does not impede the addition of a GlcNAc residue to the "3-arm" Man**4** by GnT I or subsequent structural elaborations.[36] Consistent with this mode of action, MALDI-TOF MS analysis of the N-linked glycans of IgG1 Fc expressed with 10 μM swainsonine revealed an heterogeneous spectrum of putative hybrid-type glycans indicating variable terminal β1→4-linked galactose, "bisecting" β1→4-linked GlcNAc, and a population of sialylated hybrid-type glycans (m/z = 2081.7; Figure 1C). Finally, Fc bearing complex-type glycans were generated using HEK 293T cells with no inhibitors present. MALDI-TOF MS analysis revealed biantennary complex-type glycans with variable terminal galactose (Figure 1D). This spectrum is consistent with previous observations that Fc glycosylation is highly protein-directed[20] and substantially less processed than other glycoproteins similarly expressed using the pHLSec expression vector in HEK 293T cells.[37,38]

Levels of both galactose and sialic acid in the hybrid-type spectrum were higher than those observed for the complex-type glycoforms. As sialic acid can alter the ionization efficiency of glycans in mass spectrometry,[39] we also subjected the hybrid and complex-type glycans to electrospray ionization (ESI) mass spectrometry (Figure 2). No sialylated structures were detected by ESI–MS of the glycans released from the Fc glycoform bearing complex-type glycans (Figure 2B). In contrast, the spectrum of glycans deriving from Fc expressed in the presence of swainsonine contained a prominent peak at m/z 2035.7 corresponding to a sialylated core-fucosylated hybrid-type glycan (Figure 2A).

Isomeric assignments of the hybrid-type structures were determined by negative-ion ESI MS/MS of the enzymatically released glycans. The fragmentation spectra of the most abundant species are presented in Figure 3. The m/z values of the "D-type ions", as defined by Harvey,[40] are a signature of the 6-arm. These D-type ions are annotated in the spectra and are formed by the formal loss of the 3-arm and the fucosylated di-*N*-acetylchitobiose core. Similarly, the D′-type ions, formed by cleavage of the 6-arm, reveal the cluster of mannose residues on the 6-arm. Bisecting GlcNAc residues are revealed by an abundant $[D - 221]^-$ ion at m/z 629 and the virtual absence of a D-type ion[41] (Figure 3B). The absence of an ion at m/z 306 shows that the sialic acid residue is α2→3-linked (Figure 3A).[42,43] This linkage contrasts α2→6-linked sialic acid observed in serum-derived antibodies.[44]

To assess the level of sialic acid in the hybrid-type glycans, we expressed an intact IgG1 antibody hybrid-type glycoform and subjected the fluorescently derivatized glycans to normal-phase HPLC. This analysis revealed that 20% of these swainsonine-induced hybrid-type glycans were sialylated (Figure 4A). Consistent with our MALDI–MS and ESI–MS data of IgG1 Fc glycans, no sialylated structures were observed in IgG produced in the absence of swainsonine (Figure 4B).

Swainsonine is not known to affect galactosyltransferase or sialyltransferase activity, as confirmed by the similar glycan profiles of the same glycoproteins expressed in HEK 293T cells

dx.doi.org/10.1021/ja306068g | J. Am. Chem. Soc. 2012, 134, 17554–17563

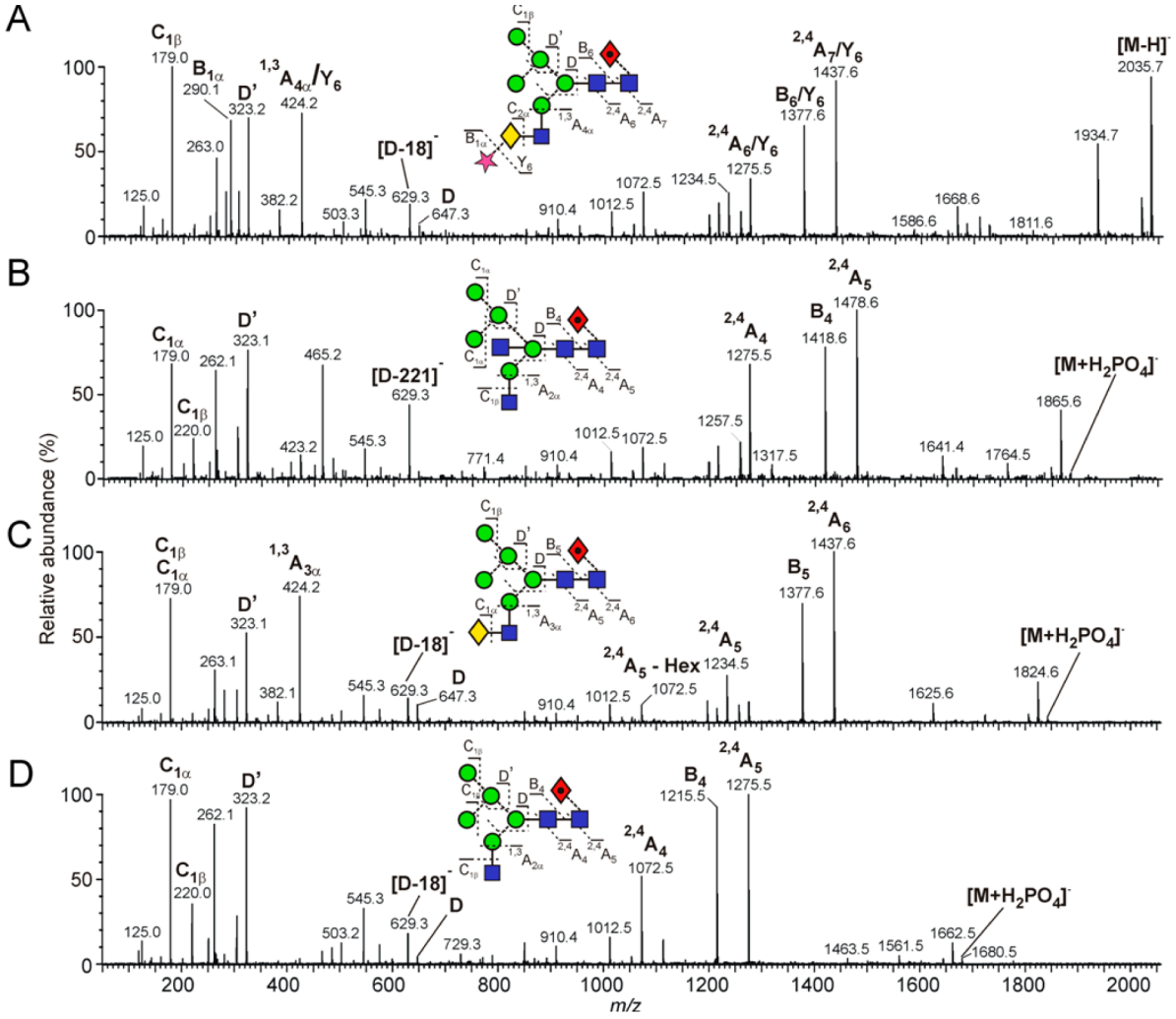

Figure 3. Negative ion fragmentation spectra of the major N-linked glycans from the hybrid-type gycoform of IgG1 Fc. Neutral glycan ions are $[M + H_2PO_4]^-$, while the sialylated glycan forms a $[M - H]^-$ ion. (A) Sialylated, fucosylated hybrid glycan ($Man_5Gal_1GlcNAc_3Fuc_1NeuNAc_1$), m/z 2035.7. (B) Bisected, fucosylated hybrid glycan ($Man_5GlcNAc_4Fuc_1$), m/z 1883.6. (C) Fucosylated hybrid glycan ($Man_5Gal_1GlcNAc_3Fuc_1$), m/z 1842.6. (D) Agalactosylated, fucosylated hybrid glycan ($Man_5GlcNAc_3Fuc_1$), m/z 1680.5. The nomenclature describing fragmentation ions follows that of Domon and Costello[45] and is distinct from the carbohydrate residue labels (Figure 1).

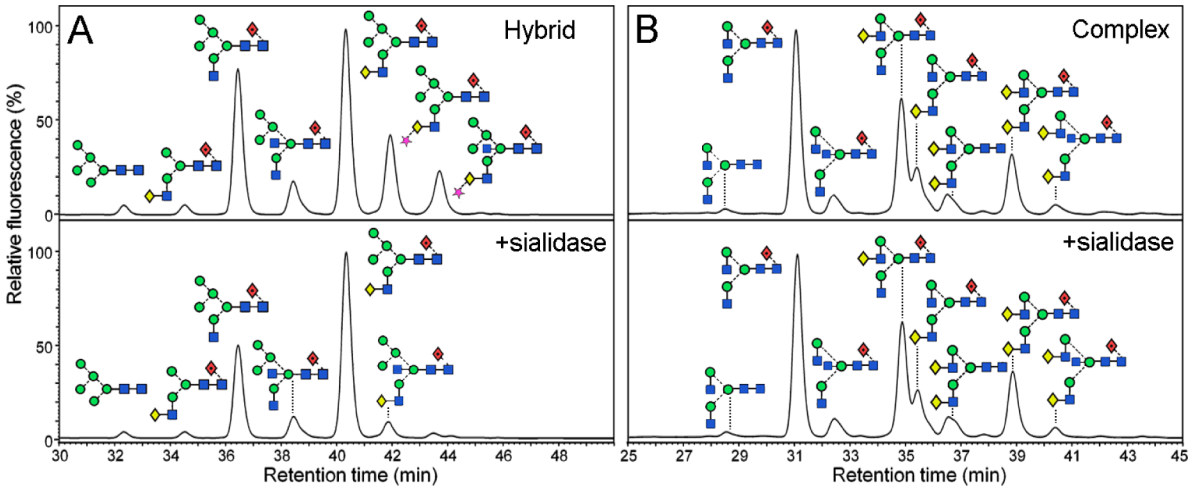

Figure 4. HPLC analysis of fluorescently labeled N-linked glycans from recombinant IgG1expressed in HEK 293T cells in (A) the presence and (B) the absence of the GnT I inhibitor, swainsonine. The lower panels show the spectra of glycans following digestion with *Arthrobacter ureafaciens* sialidase. Symbols for the structures are as described in Figure 1.

dx.doi.org/10.1021/ja306068g | J. Am. Chem. Soc. 2012, 134, 17554−17563

in the presence of swainsonine and in HEK 293T Lec36 cells that are devoid of Golgi α-mannosidase II activity.[38] Similarly, there was no evidence of increased terminal processing upon disruption of Golgi α-mannosidase II activity as compared to glycoproteins expressed in HEK 293T cells.[38] Therefore, the increased abundance of galactose and sialic acid residues in the 3-arm of the hybrid-type glycoform, as compared to the complex glycoform, may be indicative of increased steric accessibility of the Fc glycans to processing enzymes.

Thermodynamic Stability of Fc Glycoforms. One explanation for the increased 3-arm processing of the hybrid-type glycoform as compared to that of the complex-type glycan is that the accessibility of the glycans is influenced by composition and structure of the glycan−protein interface. Because of the highly processed composition of the hybrid-type glycoform, we hypothesized it would exhibit distinct glycan−protein packing interactions with altered stability. We assessed our panel of Fc glycoforms by differential scanning flourimetry (Figure 5).

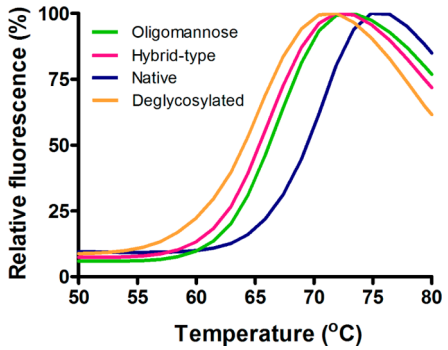

Figure 5. Thermodynamic stability of IgG1 Fc glycoforms. Single thermostability measurements of oligomannose ($Man_9GlcNAc_2$), hybrid, and complex-type glycoforms are shown. Measurements were performed in triplicate.

This analysis revealed that relative to the melting temperature (T_m) of the complex-type glycoform, the other glycoforms exhibited reduced T_m values: $Man_9GlcNAc_2$ (T_m = −2.8 ± 0.7 °C), hybrid-type glycoforms (T_m = −4.0 ± 0.7 °C), and endoglycosylated-treated Fc (−5.2 ± 1.0 °C). Therefore, in addition to reducing glycan accessibility to glycosyltransferases, the enzymatic action of Golgi α-mannosidase II, to produce complex-type glycans, is permissive for the biosynthesis of a more thermally stabilized Fc structure. We sought to investigate the structural basis for this observation by X-ray crystallography.

Structural Characterization of the Hybrid-Type Fc Glycoform. Crystallographic structures of IgG Fc have been reported for a number of glycoforms ranging from oligomannose $Man_9GlcNAc_2$, to homogeneous complex-type, and endoglycosidase-deactivated and aglycosylated states.[11,15,37,46] However, no crystallographic information is available for the hybrid-type Fc glycoform that represents the biosynthetic transition point between oligomannose and complex-type glycosylation states. We determined the crystal structure of this key intermediate (Table 1).

The hybrid-type glycoform crystallized in the primitive orthorhombic spacegroup, $P2_12_12_1$, with one homodimer in the asymmetric unit. The Cγ3 protomers were very similar in structure (0.3 Å root-mean-square deviation over 103 equivalent Cα residues) and exhibited noncrystallographic 2-fold rotational symmetry. However, the orientations of the Cγ2 protomers were arranged such that they introduced asymmetry to the homodimer, as has been frequently observed[47,48] (Figure 6A,B). The protein and carbohydrate components of the Cγ2 domain of one chain (referred to here as chain A) were largely ordered, while those from the other (chain B) exhibited higher *B*-values where some Cγ3-distal loop regions and associated glycan residues were disordered and not clearly visible in the electron density (Figure 6A).

Table 1. Crystallographic Data and Refinement Statistics

Data Collection	
beamline	BM-14
resolution range (Å)	50.0−2.36 (2.44−2.36)[a]
space group	$P2_12_12_1$
cell dimensions	
a, *b*, *c* (Å)	49.0, 72.9, 140.8
α, *β*, *γ* (deg)	90.0, 90.0, 90.0
wavelength (Å)	0.953
unique reflections	21 447 (2094)
completeness (%)	99.3 (98.7)
R_{merge} (%)[b]	9.9 (65.3)
$I/\sigma I$	16.5 (2.4)
avg redundancy	4.8 (4.5)
Refinement	
resolution range (Å)	40.0−2.36 (2.42−2.36)
no. of reflections	21 379 (1459)
R_{work} (%)[c]	21.5
R_{free} (%)[d]	26.6
rmsd[e]	
bonds (Å)	0.006
angles (deg)	1.2
molecules per asu[f]	1
atoms per asu (protein/carbohydrate/water)	3183/93/218
average *B*-factors (Å^2) (protein/carbohydrate/water)	43.2/84.7/36.8
model quality (Ramachandran plot)[g]	
most favored region (%)	99.5
allowed region	0.5

[a]Numbers in parentheses refer to the relevant outer resolution shell. [b]$R_{merge} = \sum_{hkl}\sum_i|I(hkl;i) - \langle I(hkl)\rangle|/\sum_{hkl}\sum_i I(hkl;i)$, where $I(hkl;i)$ is the intensity of an individual measurement and $\langle I(hkl)\rangle$ is the average intensity from multiple observations. [c]$R_{work} = \sum_{hkl}||F_{obs}| - k|F_{calc}||/\sum_{hkl}|F_{obs}|$. [d]$R_{free}$ is calculated as for R_{work}, but using only 5% of the data, which were sequestered prior to refinement. [e]rmsd: root-mean-square deviation from ideal geometry. [f]asu: asymmetric unit. [g]Ramachandran plots were calculated with Molprobity.[49]

The different configurations of the Cγ2 domains may arise due to differences in stabilizing crystallographic packing interactions. This hypothesis is supported by analysis of the crystalline assembly.[10] This analysis reveals that the Cγ2 domain of the more ordered chain A exhibits 37% more buried surface area with symmetry-related molecules than does the corresponding domain in chain B.

Biosynthetic Conformational Transitions. *Overall Conformation.* In chain A of our hybrid-type glycoform, we observe electron density for eight saccharide residues, corresponding to the entirety of the fucosylated oligomannose component of the hybrid-type glycan (Figure 6B). No electron density was observed for the processed 3-arm beyond Man**4**. The 3-arm is entirely solvent exposed with the nearest

dx.doi.org/10.1021/ja306068g | J. Am. Chem. Soc. 2012, 134, 17554−17563

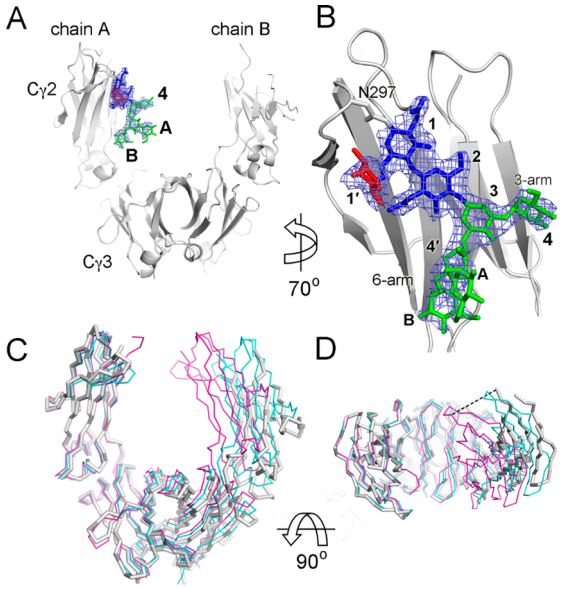

Figure 6. Crystal structure of the hybrid-type glycoform of human IgG1 Fc. (A) The Fc structure with the protein moiety shown as a gray ribbon with the N-linked glycan of N297 shown as sticks. Carbohydrate residues are colored and labeled as in Figure 1. A maximum likelihood weighted $2F_o - F_c$ electron density map is plotted around the glycan at 1σ. (B) Panel A rotated 70° with a close-up view of the protein and carbohydrate components of the Cγ2 domain from chain A of the hybrid Fc crystal structure. No electron density was observed for the processed 3-arm beyond Man**4**. (C) Overlay of the protein backbone of the hybrid (gray), oligomannose (cyan; PDB accession code 2WAH), and complex-type (pink; PDB accession code 3AVE) glycoforms. (D) The overlay in panel C rotated 90° with a dashed line corresponding to a 17 Å distance between equivalent Ser298 Cα atoms in the hybrid- and complex-type glycoforms.

component of a symmetry-related molecule located 9 Å away. While we cannot formally exclude the possibility of selective crystallization of a subset of hybrid-type glycoforms, this distance, and the large accessible volume surrounding the 3-arm, provides no evidence for such a phenomenon.

From the observation that the conformations of complex-type glycans are not influenced by the presence of fucose,[46] we suggest that the structure of the $Man_5GlcNAc_2$ component of the hybrid-type glycan reported herein is likely to resemble the $Man_5GlcNAc_2$ glycoform that occurs in the preceding stage of the pathway (Figure 1). This assertion, combined with analysis of the previously reported $Man_9GlcNAc_2$ Fc structure[47] and the series of complex-type structures by Krapp et al.,[11] now enables us to propose a model of glycan maturation during antibody biogenesis.

The folded $Man_9GlcNAc_2$ glycoform is generated following the hydrolysis of the glucose cap and consequent release from the calnexin/calreticulin folding check-point.[32] All available structures of Fc glycoforms show a conserved mode of interaction of the saccharide residues proximal to the protein attachment site. The Manβ1→4GlcNAcβ1→4GlcNAc core and the observable 3-arm residues exhibit highly similar conformations and glycan−protein packing interactions. In contrast, the 6-arm residues exhibit divergent conformations reflecting the different chemical compositions and/or surrounding environments of the glycan residues (Figure 7).

Transition from $Man_9GlcNAc_2$ to $Man_5GlcNAc_2$. The structural rearrangements that occur within the oligosaccharide when carbohydrates are modified are illustrated by the hydrolysis of terminal α1→2 mannose residues of the $Man_9GlcNAc_2$ glycoform. The Man**D3** residue in the $Man_9GlcNAc_2$ structure anchors the oligosaccharide chain to the protein surface at the junction of the Cγ2 and Cγ3 domains (Figure 7A). As the solvent accessible Man**D1** and Man**D2** residues are disordered in the crystal structure,[47] hydrolysis of Man**D3** is likely to induce the observed rearrangement of the 6-arm and cause the 6 Å shift of Man**B** (Figure 7A,B). This cleavage also results in the associated relaxation of the Man**4**′α1→6Man**3** linkage (from φ = 69°, ψ = −178°, ω = 62° to φ = 77°, ψ = 101°, ω = 30°; Figure 7A,B). Despite this movement, the Man**4**′ residue in the $Man_5GlcNAc_2$ glycoform is orientated in a direction opposite to that of complex-type structures (Figure 7C). This orientation is maintained by the presence of Man**A** and Man**B** residues of the 6-arm that sterically prevent further rotation of the Man**4**′α1→6Man**3** linkage (Figure 7B).

Transition from $Man_5GlcNAc_2$ to Hybrid-Type. The action of GnT I on $Man_5GlcNAc_2$ catalyzes the formation of hybrid-type glycans and allows downstream carbohydrate processing (Figure 1). GnT I transfers β1→2-linked GlcNAc to the Man**4** residue of the 3-arm to form the GlcNAc**5**β1→2Man**4** linkage (Figure 7B,C). As for many structures of complex-type glycoforms, we do not observe interpretable electron density for the solvated and mobile residues on this arm. Additionally, GnT I catalysis also renders the core GlcNAc residue (GlcNAc**1**) of the hybrid-type glycan susceptible to α1→6-fucosylation.[36] We observe electron density for the fucose and note the conformation closely resembles that of the complex-type glycoform (Figure 7B,C). This supports our assertion that $Man_5GlcNAc_2$ glycans are not affected structurally by fucosylation.

Formation of Complex-type Glycans. Golgi α-mannosidase II hydrolyses the α1→3-linked Man**A** and α1→6-linked Man**B** residues from the 6-arm and is dependent upon the prior activity of GnT I (Figure 1). Elimination of these residues relieves steric restraints around the 6-arm and allows the reorientation of the Man**4**′α1→6Man**3** linkage (from φ = 77°, ψ = 101°, ω = 30° to φ = 62° ψ =171°, ω = −175°; Figure 7B,C), causing close alignment of the glycan to the protein surface.

Following this rearrangement, GnT II catalyzes the transfer of β1→2-linked GlcNAc to Man**4**′, allowing the formation of hydrophobic stacking interactions between GlcNAc**5**′ and Phe243 (Figure 7C). The formation of these canonical glycan−protein interactions is consistent with the increased stability[17] (Figure 5 and Supporting Information Figure S1) and decreased enzymatic processing of the mature complex-type glycoform relative to the artificially trapped hybrid-type glycoform (Figures 1, 2, and 4). Limited downstream compositional heterogeneity of the complex-type glycoform subsequently arises from the partial transfer of galactose to terminal GlcNAc**5** and GlcNAc**5**′ residues[18] and leads to little change with respect to carbohydrate conformation or thermal stability.[11,17]

Evidence for the suppression of galactosylation and sialylation by the interaction between GlcNAc**5**′ and Phe243 is provided by the analysis of IgG from a patient with a homozygous mutation in the *Mgat2* gene.[50] *Mgat2* encodes GnT II that catalyzes the transfer of the 6-arm GlcNAc**5**′ to Man**4**′. The IgG Fc glycans isolated from the patient lacked 6-arm GlcNAc**5**′ but exhibited significantly elevated 3-arm

dx.doi.org/10.1021/ja306068g | J. Am. Chem. Soc. 2012, 134, 17554−17563

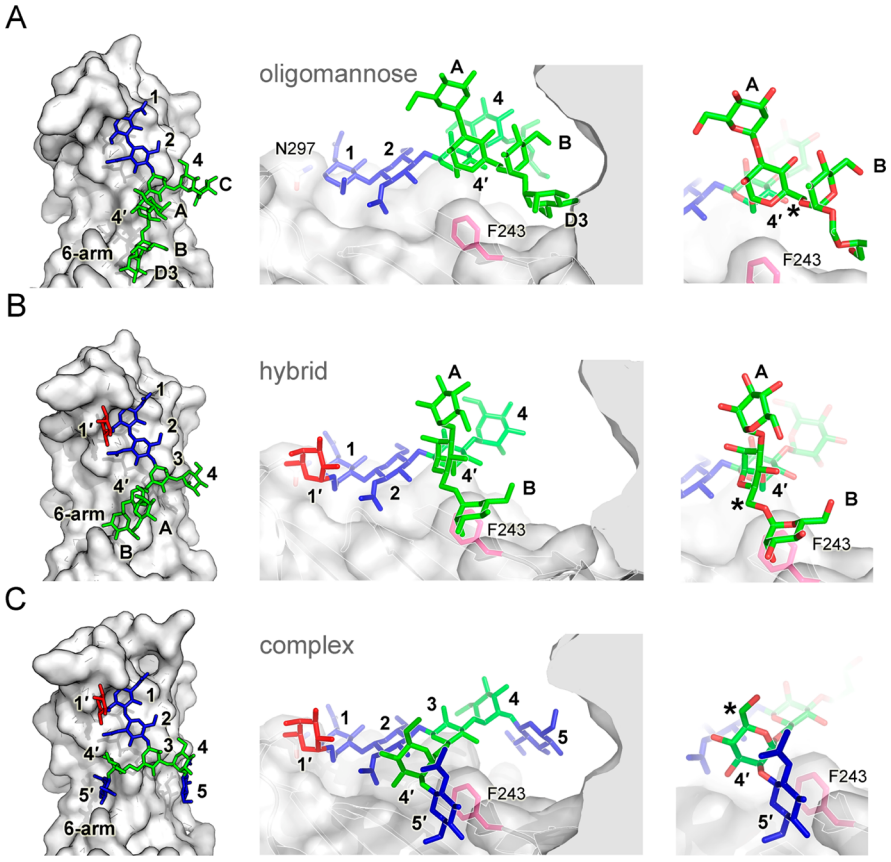

Figure 7. Structural transitions of IgG1 Fc glycans between (A) oligomannose-type (PDB accession code 2WAH), (B) hybrid-type, and (C) complex-type glycosylation (PDB accession code 3AVE), as observed by X-ray crystallography. The left-hand column displays the glycan packing against the Cγ2 domain. The central column shows a view with the 6-arm in the foreground. The right-hand column is a close-up and shows the conformational changes occurring within the 6-arm; an asterix indicates the location of the C6 carbon of the Man**4**′ residue. The protein surface is colored gray, the F243 side-chain is colored pink, and the glycan is colored as in Figure 1 except in the close-up where the oxygen atoms of mannose residues are shown in red.

processing as compared to wild-type structures with the majority of glycans containing the NeuNAc7α2→6Gal6β1→4GlcNAc**5** motif.[50] Together with our structural observations, we suggest that the action of Golgi α-mannosidase II and GnT II enhance the glycan−protein interface and limit glycosyltransferase accessibility to the 3-arm.

SUMMARY AND CONCLUSIONS

The use of glycosidase inhibitors and cell-lines with genetically modified glycan processing enzymes offers a powerful route to the isolation of glycoproteins with defined glycan structures.[34,51] These methods offer an attractive alternative to direct chemical synthesis and can be readily combined with chemoenzmatic methodologies.[3,7,8,52,53]

Analysis of isolated biosynthetic intermediates of IgG1 Fc revealed distinct differences in the susceptibility of discrete glycan states to glycosyltransferases. Specifically, we have shown by mass spectrometry that the trapped hybrid-type glycans are more readily accessible to galactosyl and sialyltransferases than are complex-type structures. The generation of hybrid-type glycoforms with increased Fc sialylation is of note given the enhanced anti-inflammatory functionality exhibited by sialylated Fc in, for example, intravenous immunoglobulin therapy.[22]

The biosynthetic intermediates also exhibited reduced stability, an important parameter in the development of antibody therapeutics.[54] Through our X-ray crystallographic analysis, we correlate this stability to structural transitions that occur during antibody biogenesis. We offer a molecular-level explanation for how stability arises from rearrangements of the glycan−protein interface. We deduce that glycan-dependent stabilization occurs during Golgi α-mannosidase II and GnT II processing, which respectively cause the relaxation of the 6-arm toward the protein surface and the formation of hydrophobic glycan−protein interfaces.

Given the promising portfolio of effector functions exhibited by IgG bearing oligomannose and hybrid-type glycans,[15,24,25,27,28] knowledge of their three-dimensional structure and defined molecular transitions provides a template to support structure-guided stabilization and optimization for the clinic.

EXPERIMENTAL PROCEDURES

Protein Expression and Purification. The Fc region of human IgG1 (residues 120−329, GenBank accession no. J00228) was cloned into the pHLSec vector[55] and transiently expressed in HEK 293T cells (ATCC number CRL-1573), GnT I-deficient HEK 293S cells,[35] and in the presence of mannosidase inhibitors to isolate glycoforms of distinct composition.[34] Transfections were performed using 2 mg of DNA per liter cell culture medium as previously described.[55] Fc bearing $Man_9GlcNAc_2$ and hybrid-type glycosylation were obtained by expression in the presence of 20 and 10 μM of the inhibitors, kifunensine[34] and swainsonine,[31] respectively (Toronto Research

dx.doi.org/10.1021/ja306068g | J. Am. Chem. Soc. 2012, 134, 17554−17563

Chemicals, Canada). Inhibitors were added at the time of transfection, and the supernatants were harvested after 5 days. IgG1 Fc glycoproteins were purified at room temperature by immobilized metal-affinity chromatography (GE Healthcare, Bucks, UK) and size exclusion chromatography using a Superdex 200 10/30 column (Amersham, Bucks, UK), in a buffer containing 150 mM NaCl and 10 mM Tris pH 8.0. Yields were typically 20 mg of purified IgG1 Fc per liter cell culture.

Plasmids encoding IgG1 b12 light and heavy chains were kindly provided by Professor Dennis Burton (The Scripps Research Institute, CA). The heavy and light chains were transiently cotransfected in HEK 293T cells in the presence or absence of 10 μM swainsonine.[31] IgG1 b12 was purified by incubation for 2 h with Protein A Sepharose (GE Healthcare, UK) at room temperature. The beads were washed with phosphate buffered saline (PBS) before elution using 0.1 M citric acid pH 3.4 followed by neutralization and size exclusion chromatography. Yields were typically 8 mg of purified IgG1 b12 per liter cell culture.

Thermodynamic Stability of IgG1 Fc Glycoforms. The thermal stability of different Fc glycoforms was assessed by differential scanning fluorimetry using a Stratagene RT PCR 305 instrument. Thermally induced unfolding of purified Fc glycoforms was monitored, in triplicate, by measuring Absorbance at 610 nm at 1.5 °C increments in the presence of Sypro Orange (Invitrogen, Paisley, UK), a fluorescent stain sensitive to hydrophobic environments.[56]

Glycan Analysis. Oligosaccharides were released from target glycoproteins with peptide-*N*-glycosidase F (New Englands Biolabs) from Coomassie blue-stained NuPAGE gels.[57] Excised bands were washed five times alternatively with acetonitrile and deionized water, and rehydrated with a 3000 units/mL of aqueous PNGase F solution. After 12 h incubation at 37 °C, the enzymatically released N-linked glycans were eluted with water. Samples were analyzed by MALDI-TOF MS with a Shimadzu AXIMA TOF^2 MALDI TOF/TOF mass spectrometer (Kratos Analytical, Manchester, UK) fitted with delayed extraction and a nitrogen laser (337 nm). Samples were cleaned on a Nafion 117 membrane (Aldrich), and then prepared for MALDI-MS by adding 0.5 μL of an aqueous solution of the glycans to the matrix solution (0.3 μL of a solution of 2,5-dihydroxybenzoic acid in acetonitrile:water; 1:1, v:v) on the stainless steel target plate and allowing it to dry at room temperature. The sample/matrix mixture was then recrystallized from ethanol.

Negative ion ESI−MS was performed with a Waters Synapt G2 traveling wave ion mobility mass spectrometer (Waters MS-Technologies, Manchester, UK).[58] Samples were dissolved in a solution of methanol:water (1:1, v:v) containing 0.5 M ammonium phosphate and introduced into the instrument with Waters thin-wall nanospray capillaries. The ESI capillary voltage was 1.2 kV, the cone voltage was 20−180 V, and the ion source temperature was 120 °C. The T-wave velocity and peak height voltages were 450 m/s and 40 V, respectively. The T-wave mobility cell contained nitrogen and was operated at a pressure of 0.55 mbar and was used to provide an additional selection stage for the fragmentation experiments. Fragmentation was performed after mobility separation in the transfer cell with a 3 mass unit selection window and with argon as the collision gas. The instrument was externally calibrated with sialylated N-glycans released from bovine fetuin. Data acquisition and processing were carried out using Waters Driftscope (version 2.1) software and MassLynx (version 4.1).

Fluorescent labeling of glycans with 2-aminobenzoic acid (2-AA) and subsequent HPLC analysis was performed as previously described.[59,60] Briefly, a buffered glycan solution was mixed with 2-AA and sodium cyanoborohydride. Labeling was achieved by incubation for 1 h at 80 °C. Excess 2-AA was removed using a Speed Amide-2 column (Systematic Instruments, UK). HPLC was carried out at room temperature in a 20 mM ammonium hydroxide solution (pH 3.9) with a linear gradient of acetonitrile and water. Exoglycosidase digestions were performed as previously described.[60]

Crystallization and Structure Determination. Crystals of IgG1 Fc bearing hybrid-type glycans were grown by sitting-drop vapor diffusion using 100 nL of protein solution (11.4 mg mL^{-1}) plus 100 nL of precipitant using the previously described semiautomated robotics of the Oxford Protein Production Facility.[61] Crystals of IgG Fc bearing hybrid-type glycans grew at 20 °C in 20% w/v PEG 3350 pH 5.5 with 0.2 M sodium/potassium phosphate after 4 days. Crystals were flash frozen by immersion in a cryoprotectant containing 25% ethylene glycol and transferred to a gaseous nitrogen stream at 100 K. Data were collected at beamline BM14 at the European Radiation Synchrotron Facility, Grenoble, France (Table 1). Diffraction data were integrated and scaled using the programs DENZO and SCALEPACK,[62] and the structure was solved by molecular replacement using the program Phaser[63] with the protein chain from a natively glycosylated IgG Fc[46] (PDB accession code 3AVE) as a search model. Five percent of reflections was randomly set aside to calculate the R_{free}. Generally, the hybrid Fc structure was refined using Refmac5 in the CCP4 suite[64] and included iterative restrained refinement with translation libration screw parametrization and incorporation of automatically generated local noncrystallographic symmetry restraints.[65,66] The molecular graphics program Coot was used for manual rebuilding,[67] and MolProbity was used to validate the model.[49] Data processing, refinement, and structure validation statistics are presented in Table 1.

Nomenclature. Throughout this work, we have adopted the system of Vliegenhart et al.[68] for labeling residues within oligomannose- and biantennary-type oligosaccharides with the additional modifications of **7** and **7′** for sialic acid, **1′** for α1→6-linked core fucose[69] (Figure 1). These residue labels are in bold-face throughout this Article. The symbolic representation of glycans follows that of Harvey et al.[33] with residues in both the schematic diagrams and the molecular graphics following the color scheme of the Centre for Functional Glycomics. Carbohydrate fragmentation ions are labeled using the Domon and Costello nomenclature[45] with an extension by Harvey.[70]

Dihedral angles were defined using the "x − 1" system for crystallography: φ = O5−C1−O−C(x)′ and ψ = C1−O−C(x)′−C(x − 1)′ for Manα1→2Man and Manα1→3Man, where x = 2 or 3, respectively; φ = O5−C1−O−C6′, ψ = C1−O−C6′−C5′, and ω = O−C6′−C5′−C4′ for Manα1→6Man linkages.[71]

■ ASSOCIATED CONTENT

Supporting Information

Atomic coordinates and crystallographic structure factors of IgG1 Fc bearing hybrid-type glycans have been deposited in the Protein Data Bank (PDB) with accession code 4B7I. This material is available free of charge via the Internet at http://pubs.acs.org.

■ AUTHOR INFORMATION

Corresponding Author

thomas.bowden@strubi.ox.ac.uk; max.crispin@bioch.ox.ac.uk

Author Contributions

⊥These authors contributed equally.

Notes

The authors declare no competing financial interest.

■ ACKNOWLEDGMENTS

This Article is dedicated to the memory of James Franz and Nigel Botting. We thank the staff of beamline BM14 at the European Synchotron Radiation Facility and Karl Harlos, Tom Walter, Weixian Lu, and David Staunton for helpful advice and technical support. We also gratefully acknowledge Prof. James Scrivens, University of Warwick, UK, for access to the Waters Synapt G2 mass spectrometer. We thank Raymond Dwek and Ian Wilson for their support. T.A.B. is a Sir Henry Wellcome Postdoctoral Fellow (Grant Number 089026/Z/09/Z) and Junior Research Fellow at University College, Oxford. M.C. is a Fellow of Oriel College, Oxford. E.Y.J. is a Cancer Research UK

Principal Research Fellow, D.I.S. is a Medical Research Council Professor of Structural Biology, K.B. was supported by an Oxford Glycobiology Institute Studentship, and A.R.A. is an MRC Career Development Award Fellow. We thank the Wellcome Trust, International AIDS Vaccine Initiative, the European Commission as SPINE2 Complexes (FP6-RTD-031220), and the Scripps Korea Antibody Institute for funding.

REFERENCES

(1) Jefferis, R. *Nat. Rev. Drug Discovery* **2009**, *8*, 226.
(2) Jefferis, R. *Expert Opin. Biol. Ther.* **2007**, *7*, 1401.
(3) Schmaltz, R. M.; Hanson, S. R.; Wong, C. H. *Chem. Rev.* **2011**, *111*, 4259.
(4) Goodfellow, J. J.; Baruah, K.; Yamamoto, K.; Bonomelli, C.; Krishna, B.; Harvey, D. J.; Crispin, M.; Scanlan, C. N.; Davis, B. G. *J. Am. Chem. Soc.* **2012**, *134*, 8030.
(5) Grayson, E. J.; Bernardes, G. J.; Chalker, J. M.; Boutureira, O.; Koeppe, J. R.; Davis, B. G. *Angew. Chem., Int. Ed.* **2011**, *50*, 4127.
(6) Payne, R. J.; Wong, C. H. *Chem. Commun.* **2010**, *46*, 21.
(7) Bernardes, G. J.; Castagner, B.; Seeberger, P. H. *ACS Chem. Biol.* **2009**, *4*, 703.
(8) Mrázek, H.; Weignerová, L.; Bojarová, P.; Novák, P.; Vaněk, O.; Bezouška, K. *Biotechnol. Adv.* **2012**, DOI: 10.1016/j.biotechadv.2012.03.008.
(9) Zou, G.; Ochiai, H.; Huang, W.; Yang, Q.; Li, C.; Wang, L. X. *J. Am. Chem. Soc.* **2011**, *133*, 18975.
(10) Krissinel, E.; Henrick, K. *J. Mol. Biol.* **2007**, *372*, 774.
(11) Krapp, S.; Mimura, Y.; Jefferis, R.; Huber, R.; Sondermann, P. *J. Mol. Biol.* **2003**, *325*, 979.
(12) Huber, R.; Deisenhofer, J.; Colman, P. M.; Matsushima, M.; Palm, W. *Nature* **1976**, *264*, 415.
(13) Deisenhofer, J. *Biochemistry* **1981**, *20*, 2361.
(14) Sondermann, P.; Huber, R.; Oosthuizen, V.; Jacob, U. *Nature* **2000**, *406*, 267.
(15) Baruah, K.; Bowden, T. A.; Krishna, B. A.; Dwek, R. A.; Crispin, M.; Scanlan, C. N. *J. Mol. Biol.* **2012**, *420*, 1.
(16) Borrok, M. J.; Jung, S. T.; Kang, T. H.; Monzingo, A. F.; Georgiou, G. *ACS Chem. Biol.* **2012**, *7*, 1596.
(17) Mimura, Y.; Church, S.; Ghirlando, R.; Ashton, P. R.; Dong, S.; Goodall, M.; Lund, J.; Jefferis, R. *Mol. Immunol.* **2000**, *37*, 697.
(18) Rudd, P. M.; Dwek, R. A. *Crit. Rev. Biochem. Mol. Biol.* **1997**, *32*, 1.
(19) Barb, A. W.; Prestegard, J. H. *Nat. Chem. Biol.* **2011**, *7*, 147.
(20) Lund, J.; Takahashi, N.; Pound, J. D.; Goodall, M.; Jefferis, R. *J. Immunol.* **1996**, *157*, 4963.
(21) Shields, R. L.; Lai, J.; Keck, R.; O'Connell, L. Y.; Hong, K.; Meng, Y. G.; Weikert, S. H.; Presta, L. G. *J. Biol. Chem.* **2002**, *277*, 26733.
(22) Nimmerjahn, F.; Ravetch, J. V. *Annu. Rev. Immunol.* **2008**, *26*, 513.
(23) Flynn, G. C.; Chen, X.; Liu, Y. D.; Shah, B.; Zhang, Z. *Mol. Immunol.* **2010**, *47*, 2074.
(24) Zhou, Q.; Shankara, S.; Roy, A.; Qiu, H.; Estes, S.; McVie-Wylie, A.; Culm-Merdek, K.; Park, A.; Pan, C.; Edmunds, T. *Biotechnol. Bioeng.* **2008**, *99*, 652.
(25) Goetze, A. M.; Liu, Y. D.; Zhang, Z.; Shah, B.; Lee, E.; Bondarenko, P. V.; Flynn, G. C. *Glycobiology* **2011**, *21*, 949.
(26) Kanda, Y.; Yamada, T.; Mori, K.; Okazaki, A.; Inoue, M.; Kitajima-Miyama, K.; Kuni-Kamochi, R.; Nakano, R.; Yano, K.; Kakita, S.; Shitara, K.; Satoh, M. *Glycobiology* **2007**, *17*, 104.
(27) Alessandri, L.; Ouellette, D.; Acquah, A.; Rieser, M.; Leblond, D.; Saltarelli, M.; Radziejewski, C.; Fujimori, T.; Correia, I. *mAbs* **2012**, *4*, 509.
(28) Yu, M.; Brown, D.; Reed, C.; Chung, S.; Lutman, J.; Stefanich, E.; Wong, A.; Stephan, J. P.; Bayer, R. *mAbs* **2012**, *4*, 475.
(29) Kornfeld, R.; Kornfeld, S. *Annu. Rev. Biochem.* **1985**, *54*, 631.
(30) Gross, V.; Tran-Thi, T. A.; Vosbeck, K.; Heinrich, P. C. *J. Biol. Chem.* **1983**, *258*, 4032.
(31) Tulsiani, D. R.; Harris, T. M.; Touster, O. *J. Biol. Chem.* **1982**, *257*, 7936.
(32) Parodi, A. J. *Annu. Rev. Biochem.* **2000**, *69*, 69.
(33) Harvey, D. J.; Merry, A. H.; Royle, L.; Campbell, M. P.; Dwek, R. A.; Rudd, P. M. *Proteomics* **2009**, *9*, 3796.
(34) Chang, V. T.; Crispin, M.; Aricescu, A. R.; Harvey, D. J.; Nettleship, J. E.; Fennelly, J. A.; Yu, C.; Boles, K. S.; Evans, E. J.; Stuart, D. I.; Dwek, R. A.; Jones, E. Y.; Owens, R. J.; Davis, S. J. *Structure* **2007**, *15*, 267.
(35) Reeves, P. J.; Callewaert, N.; Contreras, R.; Khorana, H. G. *Proc. Natl. Acad. Sci. U.S.A.* **2002**, *99*, 13419.
(36) Crispin, M.; Harvey, D. J.; Chang, V. T.; Yu, C.; Aricescu, A. R.; Jones, E. Y.; Davis, S. J.; Dwek, R. A.; Rudd, P. M. *Glycobiology* **2006**, *16*, 748.
(37) Bowden, T. A.; Crispin, M.; Graham, S. C.; Harvey, D. J.; Grimes, J. M.; Jones, E. Y.; Stuart, D. I. *J. Virol.* **2009**, *83*, 8259.
(38) Crispin, M.; Chang, V. T.; Harvey, D. J.; Dwek, R. A.; Evans, E. J.; Stuart, D. I.; Jones, E. Y.; Lord, J. M.; Spooner, R. A.; Davis, S. J. *J. Biol. Chem.* **2009**, *284*, 21684.
(39) Harvey, D. J. *Proteomics* **2005**, *5*, 1774.
(40) Harvey, D. J. *J. Mass Spectrom.* **2000**, *35*, 1178.
(41) Harvey, D. J.; Royle, L.; Radcliffe, C. M.; Rudd, P. M.; Dwek, R. A. *Anal. Biochem.* **2008**, *376*, 44.
(42) Wheeler, S. F.; Harvey, D. J. *Anal. Chem.* **2000**, *72*, 5027.
(43) Harvey, D. J.; Rudd, P. M. *Int. J. Mass Spectrom.* **2011**, *305*, 120.
(44) Dalziel, M.; McFarlane, I.; Axford, J. S. *Glycoconjugate J.* **1999**, *16*, 801.
(45) Domon, B.; Costello, C. E. *Glycoconjugate J.* **1988**, *5*, 397.
(46) Matsumiya, S.; Yamaguchi, Y.; Saito, J.; Nagano, M.; Sasakawa, H.; Otaki, S.; Satoh, M.; Shitara, K.; Kato, K. *J. Mol. Biol.* **2007**, *368*, 767.
(47) Crispin, M.; Bowden, T. A.; Coles, C. H.; Harlos, K.; Aricescu, A. R.; Harvey, D. J.; Stuart, D. I.; Jones, E. Y. *J. Mol. Biol.* **2009**, *387*, 1061.
(48) Oganesyan, V.; Damschroder, M. M.; Leach, W.; Wu, H.; Dall'Acqua, W. F. *Mol. Immunol.* **2008**, *45*, 1872.
(49) Davis, I. W.; Leaver-Fay, A.; Chen, V. B.; Block, J. N.; Kapral, G. J.; Wang, X.; Murray, L. W.; Arendall, W. B., III; Snoeyink, J.; Richardson, J. S.; Richardson, D. C. *Nucleic Acids Res.* **2007**, *35*, W375.
(50) Butler, M.; Quelhas, D.; Critchley, A. J.; Carchon, H.; Hebestreit, H. F.; Hibbert, R. G.; Vilarinho, L.; Teles, E.; Matthijs, G.; Schollen, E.; Argibay, P.; Harvey, D. J.; Dwek, R. A.; Jaeken, J.; Rudd, P. M. *Glycobiology* **2003**, *13*, 601.
(51) Beck, A.; Cochet, O.; Wurch, T. *Expert Opin. Drug Discovery* **2010**, *5*, 95.
(52) Huang, W.; Giddens, J.; Fan, S. Q.; Toonstra, C.; Wang, L. X. *J. Am. Chem. Soc.* **2012**, *134*, 12308.
(53) Hanson, S. R.; Culyba, E. K.; Hsu, T. L.; Wong, C. H.; Kelly, J. W.; Powers, E. T. *Proc. Natl. Acad. Sci. U.S.A.* **2009**, *106*, 3131.
(54) Liu, H.; Bulseco, G. G.; Sun, J. *Immunol. Lett.* **2006**, *106*, 144.
(55) Aricescu, A. R.; Lu, W.; Jones, E. Y. *Acta Crystallogr., Sect. D: Biol. Crystallogr.* **2006**, *62*, 1243.
(56) Niesen, F. H.; Berglund, H.; Vedadi, M. *Nat. Protoc.* **2007**, *2*, 2212.
(57) Küster, B.; Wheeler, S. F.; Hunter, A. P.; Dwek, R. A.; Harvey, D. J. *Anal. Biochem.* **1997**, *250*, 82.
(58) Giles, K.; Pringle, S. D.; Worthington, K. R.; Little, D.; Wildgoose, J. L.; Bateman, R. H. *Rapid Commun. Mass Spectrom.* **2004**, *18*, 2401.
(59) Neville, D. C.; Coquard, V.; Priestman, D. A.; te Vruchte, D. J.; Sillence, D. J.; Dwek, R. A.; Platt, F. M.; Butters, T. D. *Anal. Biochem.* **2004**, *331*, 275.
(60) Guile, G. R.; Rudd, P. M.; Wing, D. R.; Prime, S. B.; Dwek, R. A. *Anal. Biochem.* **1996**, *240*, 210.
(61) Walter, T. S.; Diprose, J. M.; Mayo, C. J.; Siebold, C.; Pickford, M. G.; Carter, L.; Sutton, G. C.; Berrow, N. S.; Brown, J.; Berry, I. M.; Stewart-Jones, G. B.; Grimes, J. M.; Stammers, D. K.; Esnouf, R. M.; Jones, E. Y.; Owens, R. J.; Stuart, D. I.; Harlos, K. *Acta Crystallogr., Sect. D: Biol. Crystallogr.* **2005**, *61*, 651.

(62) Otwinowski, A.; Minor, W. In *Methods in Enzymology*; Carter, C. W., Sweet, R. M., Eds.; Academic Press: New York, 1997; Vol. *276*.
(63) Storoni, L. C.; McCoy, A. J.; Read, R. J. *Acta Crystallogr., Sect. D: Biol. Crystallogr.* **2004**, *60*, 432.
(64) Collaborative Computational Project, Number 4. *Acta Crystallogr., Sect. D: Biol. Crystallogr.* **1994**, *50*, 760.
(65) Brunger, A. T.; Adams, P. D.; Clore, G. M.; DeLano, W. L.; Gros, P.; Grosse-Kunstleve, R. W.; Jiang, J. S.; Kuszewski, J.; Nilges, M.; Pannu, N. S.; Read, R. J.; Rice, L. M.; Simonson, T.; Warren, G. L. *Acta Crystallogr., Sect. D: Biol. Crystallogr.* **1998**, *54*, 905.
(66) Murshudov, G. N.; Vagin, A. A.; Dodson, E. J. *Acta Crystallogr., Sect. D: Biol. Crystallogr.* **1997**, *53*, 240.
(67) Emsley, P.; Cowtan, K. *Acta Crystallogr., Sect. D: Biol. Crystallogr.* **2004**, *60*, 2126.
(68) Vliegenthart, J. F. G.; Dorland, L.; van Halbeek, H. *Adv. Carbohydr. Chem. Biochem.* **1983**, *41*, 209.
(69) Dwek, R. A.; Lellouch, A. C.; Wormald, M. R. *J. Anat.* **1995**, *187*, 279.
(70) Harvey, D. J. *J. Mass Spectrom.* **2000**, *35*, 1178.
(71) Lutteke, T. *Acta Crystallogr., Sect. D: Biol. Crystallogr.* **2009**, *65*, 156.